# Retrieval of Nonprecipitating Liquid Water Cloud Parameters from Microwave Data: A Simulation Study

HUNG-LUNG HUANG AND GEORGE R. DIAK

*Cooperative Institute for Meteorological Satellite Studies University of Wisconsin–Madison Madison, Wisconsin*

(Manuscript received 10 January, 1991, in final form 10 June 1991)

ABSTRACT

A new microwave algorithm, analogous to the infrared "radiance-ratioing" method (Eyre and Menzel 1989) is developed to retrieve the height and "effective" fraction (defined as the product of the emissivity times the actual physical fractional coverage) of nonprecipitating water clouds using various pairs of the 20 microwave channels planned for the Advanced Microwave Sounding Unit (AMSU), an instrument slated to fly on polar-orbiting satellites beginning in 1994. The results of a simulation study are presented to provide some insights into the potentials of this technique using different AMSU channel combinations. This study suggests that the use of the oxygen channels 3 and 5 and water vapor channels 19 and 20 will produce the most accurate retrievals of liquid water cloud parameters and the highest percentage of good-quality retrievals over a range of meteorological and cloud conditions. The use of channels 1, 2, 16, and 17, which all may have a strong surface component in their measured brightness temperature, does not give optimal results chiefly because the large uncertainties in the microwave surface temperature and emissivity obscure the brightness-temperature signatures of cloud liquid water. As with the infrared radiance ratioing method (and similar $CO_2$ slicing techniques), the best retrieval of cloud parameters is for high cloud, with poorer results for those at middle and low levels.

## 1. Introduction

It has been shown that cloud liquid water plays an important role in many areas of meteorology, including showing a strong radiative impact on climate processes (Sassen et al. 1985), influencing aircraft icing encounters (Popa et al. 1986), playing a part in the development of winter storms (Reynolds and Kuciauskas 1988), and being an important element in the strategies for weather modification and cloud seeding operations (Sassen et al. 1986). It is also a significant element in degrading the propagation of radio waves.

The liquid water content of clouds has been inferred using the *Nimbus-E* Microwave Spectrometer (NEMS, Grody 1976; Staelin et al. 1976) from the Scanning Microwave Spectrometer (SCAMS, Liou and Duff 1979; Grody et al. 1980) and from ground-based systems (Snider et al. 1980; Hogg et al. 1983). All of these studies employed a water vapor– and liquid water–sensitive channel at 22.2 GHz and a window channel at 31.6 GHz to obtain the liquid water content, along with the vertically integrated water vapor amount. However, since just the single 22-GHz water vapor channel was available, the capability to retrieve a vertical distribution of cloud liquid water was practically nonexistent. Recently, Jones and Vonder Haar (1990) have applied data from the 85-GHz channels on the SSM/I, along with complementary infrared data from geostationary satellites, to estimate cloud liquid water amounts.

The Advanced Microwave Sounding Unit (AMSU), with a total of 20 channels in the microwave, represents dramatic improvements in microwave technology over the Microwave Sounding Unit (MSU) currently flying on the National Oceanic and Atmospheric Administration (NOAA) polar-orbiting satellites. Retrievals of atmospheric parameters will be substantially improved in horizontal and vertical resolution compared to those now obtainable from microwave instrumentation. Two separate radiometers (AMSU-A and AMSU-B, see Table 1 for details) comprise the AMSU platform. The primary function of the 15-channel AMSU-A (channels 1–15) is temperature sounding of the atmosphere, although three of the channels will also provide information on tropospheric water vapor, precipitation emission over ocean, sea-ice coverage, and other surface conditions. The five channels of the AMSU-B (channels 16–20) will primarily measure water vapor and liquid precipitation over land and sea. Importantly, for the first time with AMSU-B, a suite of microwave channels sensitive to the vertical distribution of water vapor will make moisture profiling of the atmosphere from a microwave instrument a routine possibility. In the clear atmosphere, the primary absorbing constit-

*Corresponding author address:* Dr. George R. Diak, CIMSS/Space Science and Engineering Center, University of Wisconsin, 1225 W. Dayton St, Madison, WI 53706.

TABLE 1. AMSU-B (channels 16–20) noise values are intended to represent the expected effective noise after averaging to AMSU-A (channels 1–15) horizontal resolution.

| AMSU | | |
|---|---|---|
| Channel number | Central frequencies (GHz) | Assumed radiometric noise (K) |
| 1 | 23.8 | 0.30 |
| 2 | 31.4 | 0.37 |
| 3 | 50.3 | 0.37 |
| 4 | 52.8 | 0.25 |
| 5 | $53.596 \pm 0.115$ | 0.27 |
| 6 | 54.4 | 0.25 |
| 7 | 54.94 | 0.25 |
| 8 | 55.5 | 0.28 |
| 9 | $v_1$ | 0.28 |
| 10 | $v_1 \pm 0.217$ | 0.40 |
| 11 | $v_1 \pm v_2 \pm 0.048$ | 0.42 |
| 12 | $v_1 \pm v_2 \pm 0.022$ | 0.63 |
| 13 | $v_1 \pm v_2 \pm 0.010$ | 0.88 |
| 14 | $v_1 \pm v_2 \pm 0.0045$ | 1.44 |
| 15 | 89.0 | 0.11 |
| 16 | 89.0 | 0.11 |
| 17 | 157.0 | 0.11 |
| 18 | $183.31 \pm 1.0$ | 0.33 |
| 19 | $183.31 \pm 3.0$ | 0.33 |
| 20 | $183.31 \pm 7.0$ | 0.33 |
| | $v_1 = 57.290344$ | |
| | $v_2 = 0.322$ | |

uents in the AMSU channels are oxygen and water vapor; however, when cloud liquid water is present, its absorption contribution may be very strong for all channels (Westwater 1972; Isaacs et al. 1985). With the AMSU response to the cloud liquid water and with the multiple channels having sensitivities to emission from different atmospheric levels, an analogous method to the multichannel $CO_2$ slicing method (Smith and Platt 1978; Menzel et al. 1983) or the similar minimum-residual methodology (Eyre and Menzel 1989) can be developed for the retrieval of the height of nonprecipitating water cloud and the effective cloud fraction.

## 2. Microwave brightness-temperature minimum-residual method

Nonprecipitating liquid water clouds usually contain drop sizes on the order of a few micrometers (see Table 2), and multiple scattering can be neglected. Thus, for this first simulation study no scattering processes were considered. In a given microwave channel the observed cloud-free brightness temperature at the top of the atmosphere may be expressed as

$$T_B^c = \epsilon_s T_s \tau(P_s, P_0) - \int_{P_0}^{P_s} T d\tau(P, P_0) + (1 - \epsilon_s)\tau(P_s, P_0) \int_{P_0}^{P_s} T d\tau(P_s, P), \quad (1)$$

where $\epsilon_s$, $T_s$, and $P_s$ are the surface emissivity, surface temperature, and surface pressure, respectively. The variable $P_0$ is the pressure at the top of the atmosphere. The variable $T$ is the profile of atmospheric temperature between the surface and top of the atmosphere, $\tau$ is transmittance, and $\tau(P_i, P_j)$ represents the transmittance between pressure levels $P_i$ and $P_j$. When nonprecipitating cloud exists within the AMSU field of view, the measured total brightness temperature at the top of the atmosphere can be given by

$$T_B = (1 - N)T_B^c + NT_B^o(P_c), \quad (2)$$

where $N$ is the effective cloud fraction, representing the product of the actual physical fractional coverage and the cloud emissivity, $T_B^c$ is the cloud-free brightness temperature, and $T_B^0$ the brightness temperature corresponding to fully overcast skies with a cloud-top pressure at $P_c$. An effective single layer of water cloud is assumed. It is also assumed that the cloud absorbs and emits but that reflection is negligible.

The brightness temperature of the cloud viewed at the top of the atmosphere is then given by

$$T_B^o(P_c) = eT_B^{Bo}(P_c) + (1 - e)T_B^c, \quad (3)$$

where $e$ is the emissivity of the water cloud and

$$T_B^{Bo} = T(P_c)\tau(P_c, 0) + \int_{P_c}^{P_0} T d\tau(P, 0). \quad (4)$$

This is the brightness temperature that would be viewed at the top of the atmosphere if the cloud were opaque. Substitution of Eqs. (1), (3), and (4) into Eq. (2) and integration by parts yields

$$T_B^c - T_B^{Bo} = -\int_{P_0}^{P_s} \tau dT + (1 - \epsilon_s)\tau_s \left[ T_s - \int_{P_0}^{P_s} T d\tau(P_s, P) \right] \quad (5)$$

and

$$T_B - T_B^c = Ne(T_B^{Bo} - T_B^c). \quad (6)$$

TABLE 2. Cloud-type characteristics.

| Model | Type | Mode radius ($\mu$m) | Liquid water content (g m$^{-3}$) | Vertical extent (km) |
|---|---|---|---|---|
| 1 | Stratus | 2.7 | 0.15 | 0.5–2.0 |
| 2 | Cumulus | 6.0 | 1.00 | 1.0–3.5 |
| 3 | Altostratus | 4.5 | 0.40 | 2.5–3.0 |
| 4 | Stratocumulus | 6.25 | 0.55 | 0.5–1.0 |
| 5 | Nimbostratus | 3.0 | 0.61 | 0.5–2.5 |

It follows from Eqs. (5) and (6), choosing two AMSU channels $v_1$ and $v_2$ that are both sensitive to liquid water cloud and where cloud and surface emissivities can be presumed to be equal, that a ratio of differences between measured total brightness temperature and calculated clear-sky brightness temperature in the two different channels $\alpha(v_1, v_2)$ can be constructed such that

$$\alpha(v_1, v_2) = \frac{T_B(v_1) - T_B^c(v_1)}{T_B(v_2) - T_B^c(v_2)} = \frac{\int_{P_c^*}^{P_s} \tau(v_1, P)dT + (1 - \epsilon_s)\tau_s(v_1)\left[T_s - \int_0^{P_s} Td\tau(v_1, P_s, P)\right]}{\int_{P_c^*}^{P_s} \tau(v_2, P)dT + (1 - \epsilon_s)\tau_s(v_2)\left[T_s - \int_0^{P_s} Td\tau(v_2, P_s, P)\right]} = \beta(v_1, v_2, P_c^*). \quad (7)$$

Given knowledge of the atmospheric temperature and moisture profile, the microwave surface emissivity $\epsilon_s$, and the surface temperature $T_s$, the term $\beta(v_1, v_2, P_c^*)$ can be calculated. The effective cloud-top pressure $P_c^*$ is then retrieved using a minimization procedure [similar to that discussed by Eyre (1989) for infrared $CO_2$ methods], which compares the measured total channel radiances to their forward modeled counterparts (radiances synthesized using the atmospheric and cloud-water profiles and surface information in appropriate models of radiative transfer). The radiative transfer equation is evaluated for the appropriate channels by summing the contributions of the brightness temperature to space from a number of atmospheric levels bounded by fixed pressure levels (in this case numbering 40), and it is convenient to calculate forward overcast and clear brightness temperature at these levels only. The cloud-top pressure is then designated as the value where

$$|\alpha(v_1, v_2) - \beta(v_1, v_2, P_c^*)| = \text{minimum}. \quad (8)$$

The surface reflection terms of Eq. (7) [terms involving $(1 - \epsilon_s)$] require the knowledge of the surface temperature and emissivity, which in practice are not always well known. Hence, for retrieval of cloud parameters, it will be shown that it is prudent to choose channel pairs whose weighting functions peak low enough in the atmosphere to have sensitivity to low-level clouds but also do not see too much of the surface so that uncertainties in $\epsilon_s$ and $T_s$ will not adversely influence the cloud retrievals. A complete investigation of the use of different channel combinations will be presented in sections 4 and 5.

In selecting the optimal value of $P_c^*$ it is also necessary to apply additional physical constraints. This retrieved cloud-top pressure must be less than the surface pressure and greater than the pressure level corresponding to −20°C, a designation of an approximate lowest temperature where water may exist in liquid phase. When no solution can be found (when $P_c^*$ is outside the range of constraints) a declaration of no retrieval is made.

Upon the successful retrieval of cloud height, the effective liquid water cloud fraction $N$ can be retrieved from Eq. (2); that is,

$$N = \frac{T_B - T_B^c}{T_B^o - T_B^c}. \quad (9)$$

## 3. Modeling the radiative effects of water cloud

Following the model outlined by Eyre (1990), the effects of cloud-liquid water in the AMSU microwave channels are included through a liquid water transmittance profile, which is unity above the cloud top and constant below the base of the cloud. Within the cloud the transmittance from space to pressure level $P_i$ is given by

$$\tau_i^c = \exp(-A_i L), \quad (10)$$

where $L$ is the total column cloud liquid water (mm), and

$$A_i = \frac{\sec\theta}{\Delta P} \sum_{j=J+1}^{i} K_j(P_j - P_{j-1}), \quad (11)$$

where $\theta$ is the surface zenith angle of the viewing path, $\Delta P$ is the total pressure depth of the cloud, and $J$ is the level of the cloud top: this is equivalent to assuming a uniform density of liquid water within the cloud. The parameter $K_j$ is the absorption coefficient for the layer, and is given in units of inverse millimeters (of water) by

$$K_j = \frac{0.0241v^2 f}{v^2 + f^2}, \quad (12)$$

with

$$f = 160 \exp[7.2(1 - 287/T_m)], \qquad (13)$$

where $T_m$ (K) is the mean temperature of the layer. The total transmittance is then obtained as the product of the cloud-water transmittance profile and the gaseous transmittance profile.

Examples are shown in Figs. 1 and 2 of the effects of cumulus cloud (a cloud with a vertical extent from 1.0 to 3.5 km with mode radius of 6.0 $\mu$m and liquid water content of 1.0 g m$^{-3}$, see Isaacs and Deblonde 1987) on the brightness temperatures of AMSU channels for dry land ($\epsilon_s = 0.95$, Fig. 1) and also ocean surface ($\epsilon_s = 0.60$, Fig. 2). For the high-emissivity land surface, the masking of the surface by cumulus cloud has the effect of lowering the brightness temperature observed at the top of the atmosphere. The magnitude of this effect depends strongly on the nature of the channel weighting function. In Fig. 1, for example, oxygen channels 6–14 see little of the lower atmosphere and surface, and the cloudy–clear differences are negligible. For the example of low-emissivity ocean surface shown in Fig. 2, the effect of the relatively low and warm cumulus cloud cover is reversed from the situation of Fig. 1, and the cloud acts to increase the brightness temperature versus the clear-air evaluation in the microwave channels. The weighting functions of AMSU 5 (an oxygen channel) and AMSU 20 (a water vapor channel) are plotted in Figs. 3 and 4 for both the cumulus-cloud and clear-sky cases. The channel weighting functions (the change of transmissivity with the change in the natural logarithm of pressure) are, in fact, probability densities indicating the relative contribution of each atmospheric level to the brightness temperature at the top of the atmosphere in a given channel. It can be seen in this figure that the presence of the cumulus cloud greatly modifies the clear-air weighting functions and produces a sharp peak in the vicinity of the cloud (600–900 mb), which makes the retrieval of effective water-cloud height feasible.

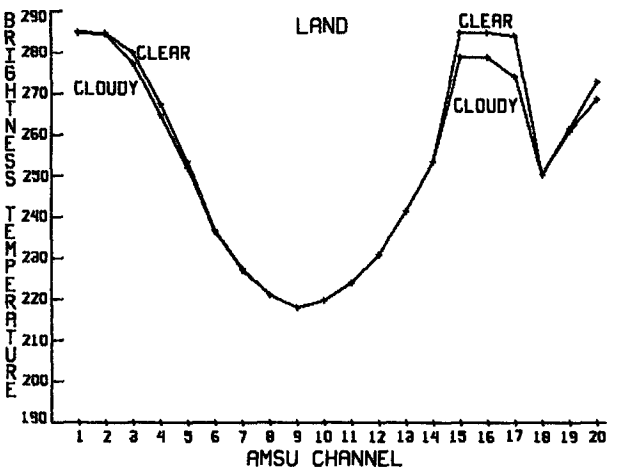


FIG. 1. Simulated top of atmosphere clear and cloudy (low cumulus cloud) brightness temperatures for AMSU channels 1–20 over a land surface.

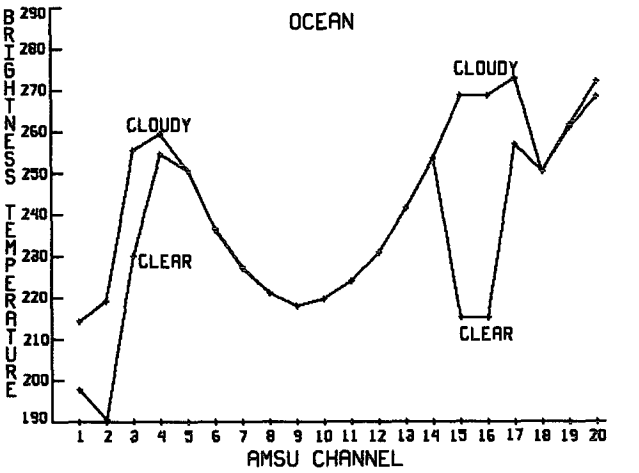


FIG. 2. Same as Fig. 1 but for a water surface.

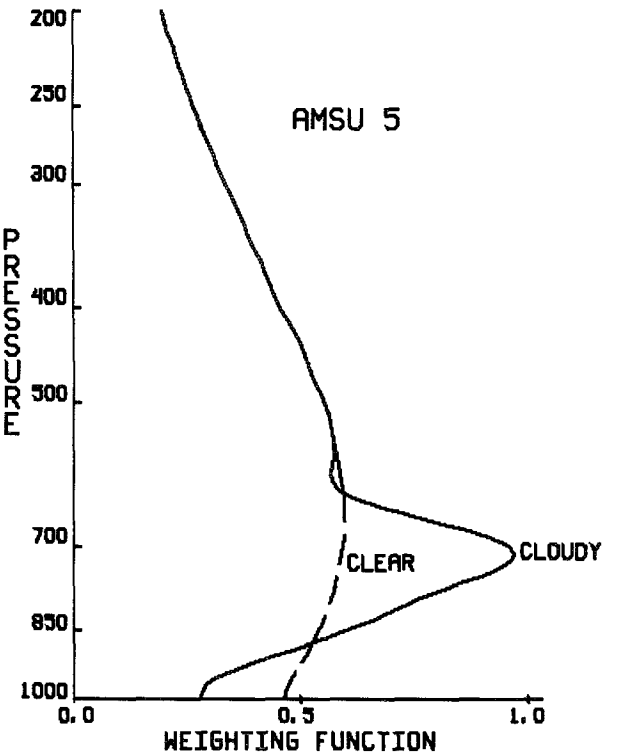


FIG. 3. Typical clear and cloudy (low cumulus cloud) vertical weighting functions (derivative of transmissivity with respect to the natural logarithm of pressure) for AMSU oxygen channel 5.

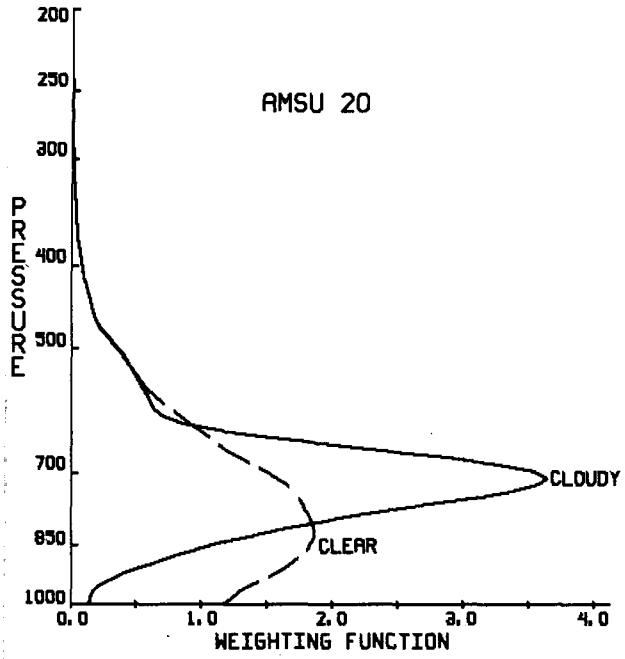


FIG. 4. Same as Fig. 3 but for water vapor channel 20.

## 4. AMSU simulation study

The theoretical development in section 2 is general enough to allow us to use any combination of AMSU channels for liquid water cloud detection, although it is advisable to select channel pairs with similar frequencies so that it can be assumed that the variation of cloud and surface emissivities across the two channels will be negligible. Here, simulations were performed for AMSU channel combinations 1 and 2, 3 and 4, 3 and 5, 4 and 5, 4 and 6, 5 and 6, 5 and 7, 6 and 7, 18 and 19, 18 and 20, and lastly channels 19 and 20. Results for this simulation will be shown in detail only for oxygen channel pair 3 and 5 (50.30 and 53.60 GHz) and water vapor pair 19 and 20 (183.31 $\pm$ 3.0 and 183.31 $\pm$ 7.0 GHz), since these two channel pairs decisively outperformed the other pairs investigated.

The simulation sequence for the retrieval of liquid water cloud height and effective cloud fraction was set up as follows. An ensemble of 400 midlatitude rawinsonde reports was taken from a global climatological dataset (Smith et al. 1974) to represent various "truth" atmospheric states. Values of the surface skin temperature required for the cloud procedures were produced by setting surface skin temperature equal to the surface air temperature from the radiosonde reports. Values of surface emissivity were fixed at 0.95 and 0.60 for land and water cases, respectively. The number of samples was expanded in each case by using each sounding with a both land and water surface emissivity value, assigning eight cloud liquid water values for each sounding ranging between 0.2 and 2.5 mm and subsequently assigning four levels of cloud-top temperature (e.g., cloud-top height) to each of these results. The final sample size produced then was the 400 soundings times two possible surface emissivities times eight levels of cloud-water amount times four levels of cloud-top temperature, or 25 600 total cloudy soundings events. Subsequently, two separate experimental sequences were performed on the 25 600 samples in order to evaluate the feasibility of the cloud-retrieval process for both totally overcast and partly cloudy conditions. In the first, the physical cloud coverage of each sample was set to unity; thus, the effective cloud fraction, as previously defined, was determined solely by the cloud emissivity (dependent on the cloud liquid water content). The AMSU cloudy brightness temperatures corresponding to these cases were calculated using the product of the gaseous-component transmittance determined by the model of Eyre and Woolf (1988) and the cloud-component transmittance as discussed in section 3. Within cloudy layers, the atmospheric relative humidity was adjusted to saturation before forward brightness-temperature calculations were performed. The second experiment was very similar, except that a cloud physical coverage ranging between 0.1 and 1.0 was randomly assigned to each of the 25 600 soundings, and the synthetic AMSU brightness-temperature data thus included the contributions of both clear and cloudy components. The effective cloud fraction to be retrieved then represented both the effects of varying emissivity and physical cloud-coverage variations. To simulate realistically the effects of instrument errors in the synthetic database, instrument noise in the AMSU channels were added to the synthetic brightness temperatures using the values given in Table 1.

In practice, we generally do not have a perfect knowledge of the state of the atmosphere and surface; therefore, the calculation of the various terms on the right-hand side of Eq. (7) and subsequent cloud retrievals will contain errors. Most often a guess of the atmospheric and surface state to be used in these calculations will come from a forecast-model prediction valid as close to the time of the satellite data as is possible. Thus, to realistically simulate a cloud-retrieval process, it must be taken into account that the estimation of the terms in Eq. (7), which rely on surface and atmospheric profile information, will be imperfect. To calculate these terms for the purpose of the cloud retrieval, Gaussian errors were added to the rawinsonde atmospheric temperature and moisture profiles with a standard deviation of 2 K and 20%, respectively. Similarly, Gaussian errors in the surface temperature and emissivity were presumed to be 2 K and 2%, respectively. It was also assumed that the forward model for calculation of the brightness temperatures from the guesses of atmosphere and surface had errors of 0.2 K in all the channels investigated.

Logistically then, in Eqs. (1) and (2), the truth (radiosonde) atmospheric profiles and surface temperature and emissivity values were used to calculate the simulated AMSU observational quantities $T_B(v_1)$ and $T_B(v_2)$ in $\alpha(v_1, v_2)$ on the left-hand side of Eq. (7). The parts of the retrieval process that rely on a priori atmospheric and surface information [all the components of the term $\beta(v_1, v_2, P_c^*)$] were calculated for each sample using the atmospheric profile and surface quantities including the errors just discussed.

## 5. Results

The AMSU cloudy brightness temperatures were simulated, and cloud-top height and effective fraction were retrieved for the 400 profiles for each combination of four cloud-top temperatures (−20°, −10°, 0°, and 10°C corresponding to high, medium, medium-low, and low cloud levels, respectively), eight total liquid water contents (0.2, 0.4, 0.6, 0.8, 1.0, 1.5, 2.0, and 2.5 mm), land- and water-surface emissivities, and overcast and partially filled field-of-view cloud conditions. The results of oxygen channel combination 3 and 5 and water vapor channel combination 19 and 20 are emphasized since these two channel pairs not only produced the best retrieval skill by a good margin but also produced the highest percentage of successful (within physical bounds) retrievals. The figures contain information on the retrievals averaged for both land and water cases for these two channel pairs. However, in Tables 3 and 4, the results from other channels are presented and the interesting differences that exist between land and water cases are indicated.

Figures 5 and 6 show the rms retrieval errors in cloud-top pressure for fully overcast conditions over both land and water surfaces using oxygen channel pair 3 and 5 (henceforth, the $O_2$ pair, Fig. 5) and water vapor channel pair 19 and 20 (henceforth, the WV pair, Fig. 6). For both pairs, the decrease of retrieval skill from high cloud to low cloud for almost all liquid water contents is evident. For high cloud and medium cloud, the WV pair outperforms the $O_2$ pair. In these higher cloud cases the errors in the guess profile of atmospheric water vapor from the top of the atmosphere to cloud level are cumulatively small and do not influence the radiative calculations much. Thus, the WV pair, with sharper vertical weighting functions and higher sensitivity to liquid water amount than the

TABLE 3. Root-mean-square (rms) accuracy in retrieval of cloud-top pressure (mb) as a function of cloud-water amount and cloud-top temperature (height) for fully overcast conditions using various AMSU channel pairs. The first line of results for a given channel pair and temperature is for retrieval over land surface. The second line, if it exists, shows where there are significant differences for retrievals over a water surface.

| | Cloud liquid water (mm) | | | | | | | | |
|---|---|---|---|---|---|---|---|---|---|
| Channel pair | 0.2 | 0.4 | 0.6 | 0.8 | 1.0 | 1.5 | 2.0 | 2.5 | |
| 19/20 | 42 | 26 | 23 | 20 | 16 | 14 | 14 | 14 | $T = -20°$ |
| | 93 | 45 | 40 | 33 | 36 | 33 | 27 | 26 | $T = -10°$ |
| | 140 | 118 | 98 | 102 | 95 | 88 | 89 | 97 | $T = 0°$ |
| | 203 | 179 | 175 | 167 | 163 | 154 | 152 | 154 | $T = +10°$ |
| 3/5 | 252 | 168 | 110 | 82 | 60 | 42 | 34 | 30 | $T = -20°$ |
| | 155 | 95 | 78 | 60 | 46 | 34 | 27 | 24 | |
| | 278 | 185 | 138 | 108 | 86 | 63 | 52 | 49 | $T = -10°$ |
| | 179 | 109 | 94 | 71 | 58 | 50 | 40 | 38 | |
| | 279 | 186 | 122 | 96 | 83 | 61 | 55 | 48 | $T = 0°$ |
| | 188 | 105 | 86 | 68 | 56 | 43 | 35 | 29 | |
| | 211 | 197 | 184 | 166 | 153 | 128 | 107 | 97 | $T = 10°$ |
| | 175 | 158 | 133 | 116 | 113 | 94 | 76 | 70 | |
| 5/6 | 155 | 110 | 109 | 68 | 48 | 51 | 41 | 41 | $T = -20°$ |
| | 232 | 164 | 148 | 122 | 109 | 112 | 98 | 49 | $T = -10°$ |
| | 257 | 207 | 178 | 160 | 143 | 134 | 125 | 115 | $T = 0°$ |
| | 212 | 212 | 201 | 185 | 190 | 175 | 159 | 166 | $T = 10°$ |
| 3/4 | 297 | 180 | 121 | 92 | 66 | 45 | 32 | 30 | $T = -20°$ |
| | 309 | 212 | 156 | 121 | 93 | 64 | 54 | 53 | $T = -10°$ |
| | 299 | 201 | 130 | 101 | 80 | 56 | 49 | 48 | $T = 0°$ |
| | 209 | 197 | 184 | 167 | 156 | 122 | 100 | 87 | $T = 10°$ |
| 4/6 | 194 | 116 | 85 | 62 | 46 | 40 | 38 | 34 | $T = -20°$ |
| | 240 | 159 | 128 | 105 | 102 | 75 | 67 | 64 | $T = -10°$ |
| | 252 | 194 | 150 | 129 | 113 | 102 | 97 | 85 | $T = 0°$ |
| | 208 | 197 | 179 | 181 | 190 | 161 | 147 | 144 | $T = 10°$ |
| 18/20 | 124 | 66 | 64 | 45 | 23 | 22 | 19 | 16 | $T = -20°$ |
| | 221 | 200 | 173 | 142 | 148 | 158 | 108 | 109 | $T = -10°$ |
| | 244 | 228 | 212 | 221 | 210 | 212 | 208 | 218 | $T = 0°$ |
| | 244 | 233 | 224 | 213 | 215 | 207 | 201 | 209 | $T = 10°$ |

TABLE 4. Same as Table 3, except for variable physical cloud fraction ranging between 0.1 and 1.0.

| | Cloud liquid water (mm) | | | | | | | | |
|---|---|---|---|---|---|---|---|---|---|
| Channel pair | 0.2 | 0.4 | 0.6 | 0.8 | 1.0 | 1.5 | 2.0 | 2.5 | |
| 19/20 | 115 | 79 | 63 | 46 | 67 | 66 | 40 | 55 | $T = -20°$ |
| | 166 | 133 | 110 | 86 | 111 | 98 | 98 | 79 | $T = -10°$ |
| | 187 | 163 | 150 | 144 | 153 | 144 | 139 | 138 | $T = 0°$ |
| | 213 | 195 | 182 | 179 | 180 | 168 | 167 | 165 | $T = 10°$ |
| 3/5 | 388 | 310 | 270 | 245 | 228 | 208 | 196 | 194 | $T = -20°$ |
| | 329 | 245 | 197 | 164 | 145 | 126 | 116 | 114 | |
| | 372 | 308 | 271 | 245 | 232 | 211 | 206 | 208 | $T = -10°$ |
| | 322 | 242 | 205 | 170 | 152 | 134 | 129 | 127 | |
| | 316 | 277 | 245 | 222 | 205 | 193 | 183 | 185 | $T = 0°$ |
| | 279 | 228 | 187 | 159 | 142 | 126 | 115 | 119 | |
| | 215 | 209 | 201 | 197 | 192 | 178 | 169 | 164 | $T = 10°$ |
| | 203 | 196 | 181 | 170 | 156 | 134 | 128 | 123 | |

$O_2$ pair, delivers the best results. For medium-low and low cloud the situation is reversed, as the effects of large relative uncertainties in the guess water vapor profile accumulate in the vertical column above the cloud top and become significant in the calculation of the transfer of microwave radiation in the water vapor channels.

As shown in Figs. 5 and 6, the WV pair retains more skill for cloud diagnosis at low cloud liquid water contents (1 mm and below) than does the $O_2$ pair. This is because of the high relative sensitivity of the 183-GHz water vapor channels to the presence of cloud liquid water versus the lower frequency $O_2$ channels.

Table 3 shows rms accuracy results (emphasizing the land surface) for retrieval of cloud-top pressure under fully overcast conditions using the $O_2$ and WV pairs and several other investigated channel pairs. When significant differences exist between land- and water-surface retrievals the accuracy values for the water retrievals are also shown in this table. Interestingly, for the $O_2$ pair, an underlying low-emissivity water surface significantly increases the skill in quantifying cloud-top pressure at all cloud levels versus the same retrievals over land. The effect is most pronounced at low total cloud liquid water amounts. This is no surprise since the signal (contrast) of cloud liquid water over a low-emissivity surface is strong, making its presence more easily detectable than over land. Similar principles have enabled the detection and quantification of cloud liquid water and rainfall over the sea surface using microwave information at only a single frequency. This situations enhances the quality of retrievals over a water surface and may in these cases make the results from microwave methods superior to that obtained by infrared sensors.

Figure 7 shows the same rms errors as shown in Fig. 6 for the WV pair but under partially filled FOV conditions (the simulated measurement radiances included a physical cloud coverage varying from 0.1 to 1.0, as

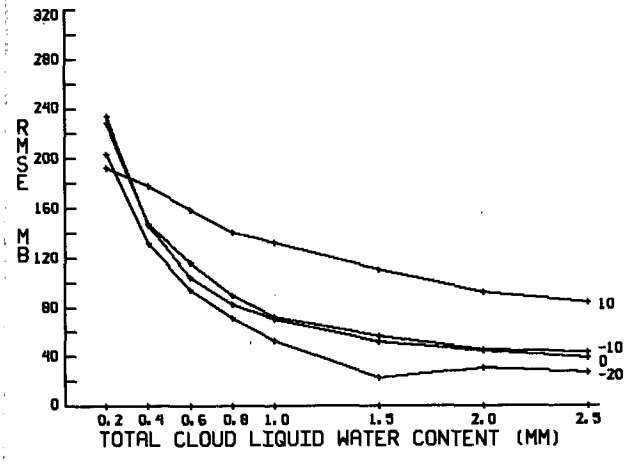


FIG. 5. Root-mean-square errors in retrieval of cloud-top pressure (mb) for land and water surfaces under fully overcast conditions over a range of cloud-top temperatures (heights) and cloud liquid water values using AMSU channels 3 and 5.

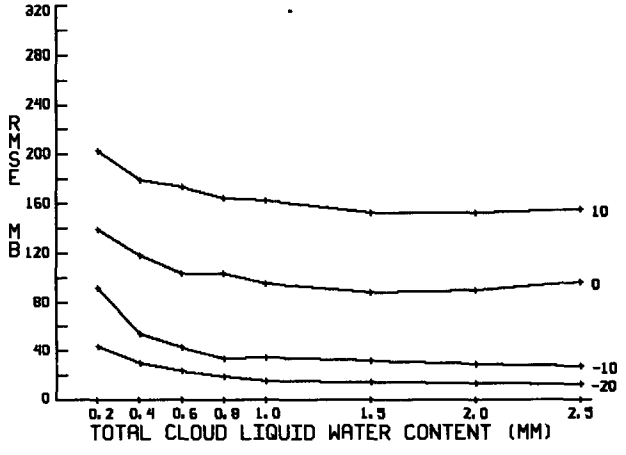


FIG. 6. Same as Fig. 5 but using channels 19 and 20.

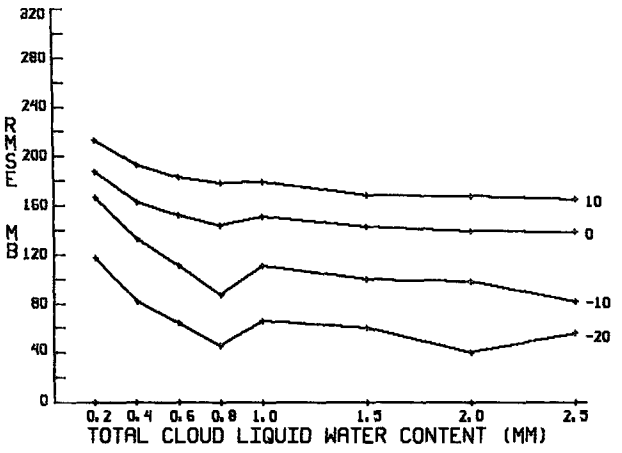


FIG. 7. Same as Fig. 6 but using simulated AMSU data in which the physical cloud coverage was varied between 0.1 and 1.0.

discussed in section 4), and a general degradation of results from totally overcast situations is evident. From comparisons of Figs. 6 and 7 it can also be seen that the degradation of cloud-height retrieval skill from overcast to partly cloudy conditions is large and most pronounced for the higher cloud types. Under partially filled FOV conditions, uncertainties in the estimation of below-cloud radiances from the guess atmospheric and surface parameters are evidenced in the retrieval system, whereas under fully overcast conditions the atmosphere and surface below the cloud are more obscured from the view of the satellite sensor. The higher the partial FOV cloud lies in the atmosphere the larger is the depth of the atmospheric column (and errors in the designation of the subcloud atmosphere) viewed by the sensor through the gaps in the cloud. It, thus, seems that the FOV resolution of microwave instruments (influencing the probability of a cloud element entirely filling an FOV) will be a crucial factor in obtaining good estimates of water-cloud height and coverage. It is worth noting that the retrieval performance of low cloud under fully overcast versus broken cloud conditions is very similar for the WV pair.

An equivalent figure to Fig. 6 ($O_2$ channels), but for partly cloudy conditions, has not been shown since the large errors in retrieved cloud-top pressure (with some exceptions to be noted) make the results only marginally useful. The $O_2$ channel weighting functions are broad in the vertical compared with their WV counterparts. Thus, with horizontal gaps in the clouds, the retrieval system sees the radiative effect of the errors in the guess atmosphere through the large atmospheric vertical extent below the cloud. Errors in designation of surface properties may also come into play.

Table 4 presents accuracy figures for the land retrievals under partially filled FOV conditions for the $O_2$ and WV pairs and also presents results for water surfaces if they differed significantly from those for land. A very interesting and unexpected feature is the improvement of retrieval results for the $O_2$ pair with increasing cloud-top temperature (decreasing cloud height) over the water surface, which is the reverse of all other examples presented for the $O_2$ and WV pairs. It appears that the proximity of cloud to the radiatively cold (low emissivity) water surface here is an asset in producing a cloud liquid water signature, outweighing the disadvantages of looking through a larger atmospheric path.

Figure 8 presents rms errors in retrieved effective cloud fraction for all four cloud heights using the WV pair cloud-height retrieval and water vapor channel 20 brightness temperature in Eq. (9) (which is used to calculate the effective cloud fraction once the cloud height has been retrieved). The response of the retrieval of effective cloud fraction with varying cloud temperature and amount of liquid water is similar to that of cloud height. Retrieval accuracy is the best for high and middle clouds, and degrades as the cloud top is lower in the atmosphere.

## 6. Discussion

These simulated results demonstrate that this microwave minimum-residual method, using channels that will be available with the launch of the AMSU instrument, will be effective in retrieving water-cloud height and amount for mid- and upper-level water clouds. The experiments predict that the best results for fully overcast conditions will be obtained by use of the oxygen channel pair 3 and 5 (i.e., the third- and fifth-lowest sounding temperature channels) and the water vapor channel pair 19 and 20 (i.e., the second and third lowest sounding water vapor channels). These combinations both give consistently reasonable

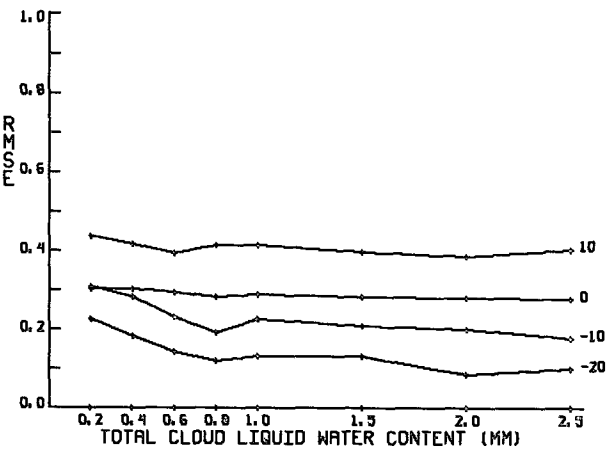


FIG. 8. Root-mean-square errors in retrieval of effective cloud fraction for land and water surfaces and various cloud-top temperatures (heights) and cloud liquid water values using AMSU channels 19 and 20.

results under overcast conditions, with somewhat better performance obtained with the $O_2$ channel pair. Other channel pairs may also produce reasonable results, as demonstrated in Table 3. The superiority of the WV pair over the $O_2$ pair under partially filled cloud conditions, however, is very interesting and important to note. Because of the high horizontal resolution of the WV versus $O_2$ channels (approximately 15 versus 40 km at nadir), we foresee that the WV pair will have a higher success rate in observing fully cloud-covered FOVs and will be more reliable overall than the $O_2$ pair, whose accuracy degrades very rapidly under partially filled FOV conditions due to the broadness of the channel vertical weighting functions. The results obtained here are very similar in quality to those obtained using infrared satellite information in a parallel method developed by Eyre and Menzel (1989). This is not at all surprising since the new technology evident in the AMSU will provide channel vertical weighting functions in the microwave that rival their infrared counterparts in vertical resolution.

Errors in the calculated brightness temperatures from errors in assumed atmospheric conditions propagate through into errors in the retrieval of cloud parameters. For the same reason, errors in surface emissivity and skin temperature are likely to degrade the retrieval, provided that the channel pair views the lower atmosphere and surface. In both oxygen and water vapor microwave absorption regions the best results were obtained with channels that have weighting function peaks in the lower atmosphere but not window channels that see too much of the surface (and thus respond to errors in designation of surface properties and at the same time lose atmospheric sensitivity). It can be noted that error effects will be less pronounced if a more accurate temperature and moisture profile and surface skin temperature and emissivity can be used.

The poor performance of all the channel pairs for low-level cloud is not surprising. At these low levels the cumulative radiative effects of uncertainties in both the atmospheric temperature and water vapor profiles influence the retrieval accuracy and errors in the surface temperature and emissivity may also enter the retrieval process due to the proximity of the surface.

The method discussed here relies on a number of assumptions, which under certain observing conditions may not be valid. First, only nonprecipitating clouds are considered. For the case of precipitating clouds, the effects of scattering in the microwave region will need to be included, or more likely, precipitating clouds will need to be screened out of the retrieval process by using the microwave data or complementary information. Second, an effective single layer of water cloud has been assumed. The problem of multilayer cloud will require additional study. The final assumption is the presumption of a uniform density of liquid water within the cloud. The simulation study reported on here has used synthetic data. It has been possible to simulate future instrumentation and to compare the behavior and error characteristics of different channel combinations (in a way that is almost impossible with real data) and to develop and test the feasibility of the methods before real data from the instrument is available. In subsequent research we plan to upgrade the realism of our simulations by using three-dimensional fields of cloud liquid water from atmospheric microphysical and dynamical prediction models to further explore the retrieval of cloud liquid water properties from the AMSU.

*Acknowledgments.* This research was supported by NASA Grant NCC8-12 in cooperation with the Marshall Space Flight Center, Huntsville, Alabama. Thanks go to two anonymous reviewers whose constructive comments were very helpful in improving the content and style of this manuscript.

## REFERENCES

Eyre, J. R., 1989: Inversion of cloudy satellite sounding radiances by nonlinear optimal estimation: Theory and simulation for TOVS. *Quart. J. Roy. Meteor. Soc.*, **115,** 1001–1026.

——, 1990: The information content of data from satellite sounding systems: A simulation study. *Quart. J. Roy. Meteor. Soc.*, **116,** 401–434.

——, and H. M. Woolf, 1988: Transmittance of atmospheric gases in the microwave region: A fast model. *Appl. Optics,* **27,** 3244–3249.

——, and W. P. Menzel, 1989: Retrieval of cloud parameters from satellite sounder data: A simulation study. *J. Appl. Meteor.*, **28,** 267–275.

Grody, N. C., 1976: Remote sensing of atmospheric water content from satellites using microwave radiometry. *IEEE Trans Antennas Propag.*, AP-**24,** 155–162.

——, A. Gruber, and W. C. Shen, 1980: Atmospheric water content over the tropical Pacific derived from the *Nimbus-6* scanning microwave spectrometer. *J. Appl. Meteor.*, **19,** 986–996.

Hogg, D. C., F. O. Guiraud, J. B. Snider, M. T. Decker, and E. R. Westwater, 1983: A steerable dual-channel microwave radiometer for measurement of water vapor and liquid in the troposphere. *J. Climate Appl. Meteor.*, **22,** 789–806.

Isaacs, R. G., and G. Deblonde, 1987: Millimeter wave moisture sounding: The effect of clouds. *Radio Sci.*, **22,** 367–377.

——,——, R. D. Worsham, and M. Livshits, 1985: Millimeter wave moisture sounder feasibility study: The effect of cloud and precipitation on moisture retrievals. AFGL Tech. Rep. AFGL-TR-85-0040.

Jones, A. S., and T. H. Vonder Haar, 1990: Passive microwave remote sensing of cloud liquid water over land regions. *J. Geophys. Res.*, **95,** 16 673–16 683.

Liou, K.-N., and A. D. Duff, 1979: Atmospheric liquid water content derived from parameterization of *Nimbus-6* scanning microwave spectrometer data. *J. Appl. Meteor.*, **18,** 99–103.

Menzel, W. P., W. L. Smith, and T. R. Stewart, 1983: Improved cloud motion wind vector and altitude assignment using VAS. *J. Climate Appl. Meteor.*, **22,** 377–384.

Popa, F., A. Ingrid, J. A. Schroeder, and M. T. Decker, 1986: Ground-based detection of aircraft icing conditions using microwave radiometers. *IEEE Trans. Geosci. Remote Sens.* **GE-24,** 975–982.

Reynolds, D. W., and A. P. Kuciauskas, 1988: Remote and in situ observations of Sierra Nevada winter mountain clouds: Rela-

tionships between mesoscale structure, precipitation and liquid water. *J. Appl. Meteor.*, **27,** 140–156.

Sassen, K., R. M. Rauber, and J. B. Snider, 1986: Multiple remote sensor observations of supercooled liquid water in a winter storm at Beaver, UT. *J. Climate Appl. Meteor.*, **25,** 825–834.

——, K.-N. Liou, S. Kinne, and M. Griffin, 1985: Highly supercooled cirrus cloud water: Confirmation and climatic implications. *Science,* **227,** 411–412.

Smith, W. L., and C. M. Platt, 1978: Comparison of satellite deduced cloud heights with indications from radiosonde and ground-based laser measurements. *J. Appl. Meteor.*, **17,** 1796–1802.

——, H. M. Woolf, P. G. Abel, C. M. Hayden, M. Chalfant, and N. Grody, 1974: *Nimbus-5* sounder data processing system part I: Measurement characteristics and data reduction procedures. NOAA Tech. Memo., NESS 57.

Snider, J. B., F. O. Guiraud, and D. C. Hogg, 1980: Comparison of cloud liquid content measured by two independent ground-based systems. *J. Appl. Meteor.*, **19,** 577–579.

Staelin, D. H., K. F. Kunzi, R. L. Pettyjohn, R. K. L. Poon, R. W. Wilcox, and J. W. Waters, 1976: Remote sensing of atmospheric water vapor and liquid water with the *Nimbus-5* microwave spectrometer. *J. Appl. Meteor.*, **15,** 1204–1214.

Westwater, E. D., 1972: Microwave emission from clouds. NOAA Tech. Rep., ERL 219-WPL 18.